



# Exclusive formation of stereocomplex crystallites in PLLA/PDLA (50/50) blends by the addition of a plasticizer

Neimatallah Hosni Mohammed Mahmoud<sup>1</sup> · Hideaki Takagi<sup>2</sup> · Nobutaka Shimizu<sup>1</sup> · Noriyuki Igarashi<sup>2</sup> · Shinichi Sakurai<sup>1</sup>

Received: 2 March 2024 / Revised: 22 April 2024 / Accepted: 23 April 2024 / Published online: 24 May 2024  
© The Society of Polymer Science, Japan 2024

## Abstract

This study examined the effects of loading amounts of a biobased plasticizer, namely, organic acid monoglyceride (OMG), on the formation of homocrystals (HCs) and stereocomplex crystals (SCs) in PLLA/PDLA (50/50) blends by means of differential scanning calorimetry (DSC), wide-angle X-ray diffraction (WAXD) and polarized optical microscopy (POM) observations. OMG at different concentrations was added to the PLLA/PDLA (50/50) blend from 0.5 to 5% in 0.5% increments. The addition of OMG was found to enhance SC formation while suppressing HC formation in both nonisothermal and isothermal experiments. The total suppression of HC formation and exclusive SC formation was achieved in the specimens with OMG contents higher than 3% after isothermal crystallization at 170 °C for 5 h. This result was confirmed by WAXD measurements of the specimens with 4 and 5% OMG, where only SC diffraction peaks were observed. In addition, the degree of crystallinity was found to be the same for the specimens with 0 and 5% OMG crystallized at 170 °C for 5 h. These findings imply that not only did the SC form exclusively but also that the presence of OMG actively accelerated its crystallization.

## Introduction

Biodegradable polymers, particularly poly(lactic acid) (PLA), have garnered significant attention in recent years owing to their sustainable and environmentally friendly nature. PLA is produced from readily available and renewable resources such as corn, wheat potato starch, or sugarcane [1]. In addition, its end-of-life treatment through composting produces carbon dioxide and water, both of which are nontoxic to the environment [2]. Nevertheless, processing PLA, under conventional conditions, restricts its industrial and commercial applications due to its slow

crystallization rate, low crystallinity, and poor thermal resistance [3–5]. There are two enantiomeric forms of PLA, poly(L-lactic acid) (PLLA) and poly(D-lactic acid) (PDLA), which have similar chemical properties but different steric structures. Ikada et al. first reported the formation of stereocomplex crystals (SCs) by combining equal amounts of PLLA and PDLA and the resulting SC had a melting temperature ( $T_m$ ) about 50 °C higher than that of homocrystals (HCs) formed by either PLLA or PDLA component [6]. While the melting temperature for HC is about 170 °C–180 °C, the melting temperature of SC is approximately 230 °C [7]. The higher melting temperature of SC leads to better thermal properties, prompting the expansion of PLA applications [8–10]. Thus, the enhancement of stereocomplexation in PLA was the aim of many studies by different methods, such as the addition of cellulose microcrystals [11], nanosilica [12], or poly(methyl methacrylate) (PMMA) [13]. Our previous study [14] sought to promote SC formation in a 50/50 blend of PLLA/PDLA by the isothermal crystallization for a prolonged duration (5 h) at a temperature close to the  $T_m$  of HC, that is, crystallization temperature  $T_c = 170$  °C. The initial assumption was that only SC would form at such a high  $T_c$  and that the long duration would allow the enhancement of its

**Supplementary information** The online version contains supplementary material available at <https://doi.org/10.1038/s41428-024-00919-4>.

✉ Shinichi Sakurai  
shin@kit.ac.jp

<sup>1</sup> Department of Biobased Materials Science, Kyoto Institute of Technology, Kyoto 606-8585, Japan

<sup>2</sup> High Energy Accelerator Research Organization (KEK), Tsukuba, Ibaraki 305-0801, Japan

crystallizability. However, the long isothermal crystallization duration resulted in HC formation, and its melting temperature was remarkably high at about 188 °C.

On the other hand, various studies have focused on improving the properties of PLA, not only by stereocomplexation but also by plasticization using different materials such as poly(ethylene glycol) (PEG) [15], poly(propylene glycol) (PPG) [16], oligomeric lactic acid (OLA) [17], citrate ester [18] and partial fatty acid ester [19]. Being biodegradable, environmentally safe, and nontoxic are important attributes of any PLA additive to sustain its biodegradability for environmental purposes. Consequently, combining both stereocomplexation and plasticization is a promising approach for enhancing the crystallizability of PLA. Although the expected plasticizer effect of melting point depression may subsequently reduce the thermodynamic driving force for crystallization, a plasticizer can effectively enhance polymer crystallinity. This may be due to the ability of the plasticizer to decrease the activation energy for crystallization [3, 20]. This was further demonstrated by our research group in a reported work investigating the effects of a special biobased plasticizer, namely, organic acid monoglyceride (OMG), on the crystallization of PLLA [21, 22]. Therefore, this study examined the effects of loading amounts of OMG on both HC and SC formation in a PLLA/PDLA (50/50) blend through experimental techniques, including differential scanning calorimetry (DSC), wide-angle X-ray diffraction (WAXD) and polarized optical microscopy (POM) observations. This study provides a comprehensive understanding of the crystallization behavior of both HC and SC in PLLA/PDLA (50/50) blends under the influence of different contents of OMG. The findings presented here not only contribute to the understanding of PLA crystallization but also pave the way for the development of advanced, sustainable materials with tailored properties.

## Experimental section

### Materials

The polymers used in this study were PLLA, obtained from NatureWorks LLC, USA (grade 2500 HP); and PDLA, obtained from Purac, Netherlands (grade D130). Table 1 summarizes the material characterization. OMG used as a plasticizer was produced from vegetable oil by Taiyo Kagaku Co., Ltd., under the commercial name Chirabasel VR (see Scheme 1 for the chemical structure) [23]. It is a “fatty acid ester surfactant” with a molecular weight of 500 and a melting temperature of 67 °C (measured by DSC). OMG comprises an organic acid as succinic acid and a saturated fatty acid as a stearic acid, and one of its main functions as an emulsifier is to improve the dispersibility of sugar and cocoa in food products.

**Table 1** Materials characterization

	PLLA	PDLA
Code	2500 HP	D130
Optical Purity	99.5%	>99.5%
Number-average molecular weight ( $M_n$ ) (GPC) <sup>*1</sup>	$1.74 \times 10^5$	$1.41 \times 10^5$
$M_w/M_n$ (GPC)	2.22	2.03

<sup>\*1</sup> The GPC column was calibrated using the standard polystyrene with chloroform as eluent at room temperature

### Specimen preparation

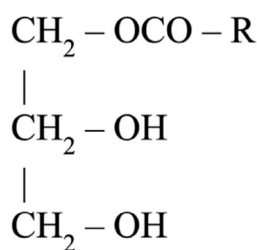
Film specimens were prepared by solution casting using dichloromethane (DCM) as solvent at a 5% (w/v) polymer concentration. A 50/50 mixture of PLLA and PDLA pellets was weighed, with the chosen OMG percentage of the total weight, and then the solvent was added. The mixtures were stirred overnight before being cast in a 5-cm diameter Petri dish for solvent evaporation at room temperature. The added percentages of OMG varied from 0.5 to 5% with a 0.5% increment, resulting in a total of eleven specimens denoted by LDx, where x is the percentage of OMG in the PLLA/PDLA (50/50) blend specimen.

### DSC measurements

DSC measurements were carried out using NETZSCH DSC214 Polyma (NETZSCH GmbH & Co. Holding, Germany) under a nitrogen atmosphere. The apparatus was calibrated using indium, zinc, bismuth, and tin as references prior to measurement. For the nonisothermal DSC, the specimens were heated from 25 °C to 250 °C at a heating rate of 10 °C/min and maintained for 5 min to erase their thermal history before being cooled down to 25 °C at a rate of 10 °C/min. The second heating run was conducted from 25 °C to 250 °C at a rate of 10 °C/min. For isothermal crystallization, the specimens were heated from 25 °C to 250 °C at a heating rate of 10 °C/min and maintained for 5 min to erase the thermal history during the casting process. Then, they were quenched to a given  $T_c$  with a cooling rate of approximately 50 °C/min and isothermally maintained for different durations. Afterward, the specimens were heated to 250 °C to evaluate the melting temperatures after isothermal crystallization. Notably, the specimens were renewed for each DSC measurement to avoid unfavorable thermal degradation of the polymers.

### WAXD Measurements

Time-resolved WAXD measurements were performed using synchrotron radiation as the X-ray source at beamlines BL-6A and BL-10C of the Photon Factory at KEK



R: substituent group with  
380 molecular weight

**Scheme 1** Chemical structure of OMG

(High-Energy Accelerator Research Organization) in Tsukuba, Japan. The wavelength of the incident X-ray beam was 0.15 nm. The examined specimens were LD3, LD4, and LD5, in addition to LD0 that was examined under the same conditions used in our previous study [14]. The specimens were positioned in an aluminum cell connected to a thermosensor to monitor their temperature throughout the measurement duration. The cell diameter and thickness were 4 mm and 1 mm, respectively. To seal the specimens in the cell, polyimide (Kapton) tape (Nitto Denko Corporation, Osaka, Japan) was used. To follow the same conditions used for the DSC measurements, two heater blocks were used to achieve the temperature jump from 250 °C to 170 °C. The specimens were melted at 250 °C for 5 min before being immediately transferred to the second heater block, maintained at  $T_c = 170$  °C. WAXD measurements were performed while ensuring that the temperature stabilized at 170 °C within a relatively short period (1–3 min) and that the temperature fluctuations during the measurements were within  $170$  °C  $\pm$  0.5 °C. The magnitude of the scattering vector ( $q$ ) was calibrated by using standard polyethylene.  $q$  is defined as  $q = |\mathbf{q}| = (4\pi/\lambda) \sin(\theta/2)$ , where  $\lambda$  and  $\theta$  are the wavelength of the X-ray and the diffraction angle, respectively. Two-dimensional wide-angle X-ray diffraction (2D-WAXD) images were recorded every 5 s with an X-ray exposure time of 4 s on Pilatus 100 K (DECTRIS Ltd., Switzerland), for BL-6A, and Pilatus 200 K (DECTRIS Ltd., Switzerland), for BL-10C, as the two-dimensional detectors. The one-dimensional WAXD profiles were obtained by taking the sector average of the 2D-WAXD images.

### POM observations

POM observations were conducted using a Nikon Eclipse Ci-POL POM instrument equipped with a Linkam THMS600 hot stage (Linkam Scientific) to observe the growth of spherulites at  $T_c = 170$  °C. The examined specimens were LD1, LD2, LD3, LD4, and LD5, in addition to LD0, which

was already examined in our previous study [14]. The specimens were positioned between two glass cover slips and melted at 250 °C for 5 min before being quenched to 170 °C at a cooling rate of 110 °C/min. Then, they were isothermally maintained for 5 h before being heated to 250 °C to observe the fading of spherulites.

## Results and discussion

### Non-isothermal DSC measurement

Figure 1a shows the first cooling run, from 250 °C to 25 °C, which was followed by the second heating run from 25 °C to 250 °C, as shown in Fig. 1b. The second heating run shows typical thermal transition signals: glass transition temperature ( $T_g$ ), cold crystallization temperature ( $T_{cc}$ ), and two distinct melting peaks  $T_{m,HC}$  and  $T_{m,SC}$ , ascribed to the melting of HC (at lower temperatures) and SC (at higher temperatures), respectively. The increase in the OMG content in the specimens had a suppressing effect on all the  $T_g$ ,  $T_{cc}$ , and  $T_m$  values, shifting them to lower temperatures. It also led to the appearance and growth of crystallization peaks during the cooling run, clearly observed in specimens LD3–LD5. This indicates the accelerating effect of OMG on crystallization, specifically stereocomplexation, which precedes HC formation when quenched from the melt [24]. Moreover, the increase in OMG content in the specimens promoted the formation of SC over the formation of HC. This was evidenced by the shrinking of the HC melting peak simultaneously observed with the expansion of that of SC as the OMG content increased in the specimens. Table S1 in the supporting information indicates that the degree of crystallinity of HC ( $\phi_{HC}$ ) decreased from 44.5% for LD0 to 11.7% (–32.8%) for LD5. On the other hand, the degree of crystallinity of SC ( $\phi_{SC}$ ) increased from 9.4% to 37.3% (+28%) for LD0 and LD5, respectively. This increase in  $\phi_{SC}$  is accompanied by a larger crystallization peak at a higher temperature, as observed in Fig. 1a, indicating accelerated stereocomplexation that may hinder the HC formation due to the suppression of the crystallization temperature of HC. Note here that  $\phi_{HC}$  and  $\phi_{SC}$  were calculated using the following equations,

$$\phi_{HC} = \frac{\Delta H_{m,HC}}{\Delta H_{m,HC}^{\circ}} \quad (1)$$

$$\phi_{SC} = \frac{\Delta H_{m,SC}}{\Delta H_{m,SC}^{\circ}} \quad (2)$$

$$\text{Total Crystallinity} = \phi_{HC} + \phi_{SC} \quad (3)$$

where  $\Delta H_{m,HC}^{\circ}$  and  $\Delta H_{m,SC}^{\circ}$  are the enthalpies of fusion of 100% crystal for HC and SC, taken as 93 Jg<sup>–1</sup> [25] and

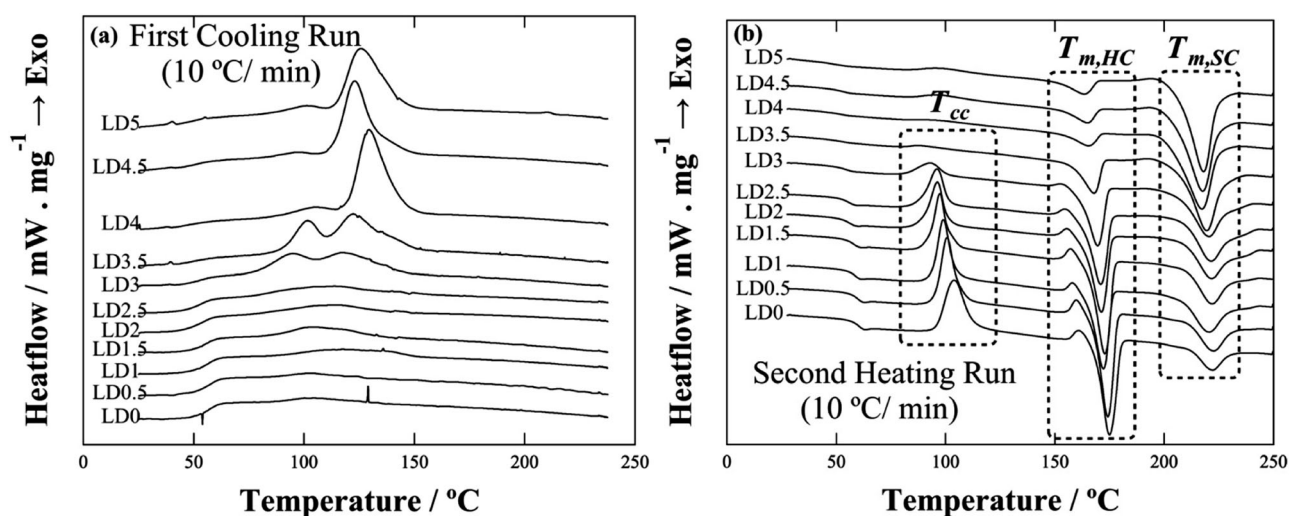


**Fig. 1** **a** First cooling and **b** second heating runs for the PLLA/PDLA (50/50) blend with different contents of OMG. LD $x$  indicates the blend specimen with an OMG content of  $x\%$

142 Jg<sup>-1</sup> [26], respectively; and  $\Delta H_{m,HC}$  and  $\Delta H_{m,SC}$  were calculated by integrating the melting peaks of HC and SC, respectively. Additionally, Table S1 contains the detailed results of the nonisothermal DSC measurements for both HC and SC for all the specimens ( $T_m$ ,  $\Delta H_m$ ,  $\phi_{HC}$  and  $\phi_{SC}$ ).

The values of  $T_g$ ,  $T_{cc}$  and  $T_m$ , obtained from the second heating DSC run are plotted in Fig. 2, in addition to the estimated values of  $T_g$ , calculated using Eq. (4) to examine the role of OMG as a plasticizer.

$$T_{g(PLLA/PDLA+OMG)}(K) = \left(1 - \frac{\text{wt}\% \text{ of OMG}}{100}\right) \times T_{g(PLLA/PDLA)}(K) \quad (4)$$

$T_g$  decreased linearly with increasing the OMG content in the specimens. However, it did not follow the estimated  $T_g$  and a significant deviation was observed, which indicates the inadequate molecular dispersion of the OMG in the specimens and its partial aggregation.

Both  $T_{m,HC}$  and  $T_{m,SC}$  decreased linearly with increasing the OMG content.  $T_{cc}$  followed a similar trend, decreasing with increasing the OMG content. However, for LD4, LD4.5, and LD5,  $T_{cc}$  peaks were not noticeable (Fig. 1b), and their crystallization peaks increased during the first cooling run (Fig. 1a). This indicates the accelerating effect of OMG on crystallization.

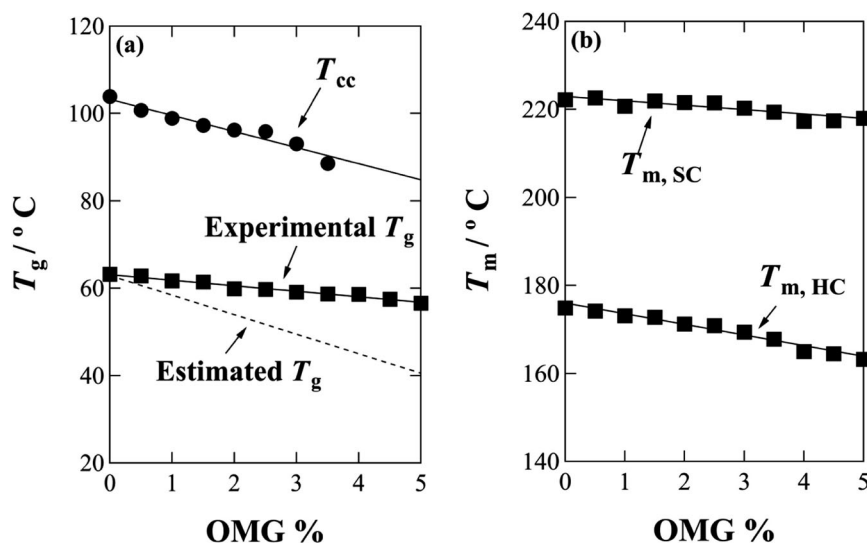
### Isothermal DSC measurements of the PLLA/PDLA (50/50) blend specimens

The isothermal DSC measurements were conducted for all the specimens at 170 °C for 5 h. The same experimental conditions (both the duration and  $T_c$ ) were used in our

previous work [14] to ensure the completion of the crystallization process, taking into consideration the slow crystallization rate of PLA [27]. For  $T_c = 170$  °C, this temperature is of interest because of its proximity to the  $T_m$  of the HC. Since we proved that HC can form at such a high  $T_c$  after about 70 min [14], our next step was to examine the effect of the plasticizer on both SC and HC formation under the same conditions. Figure 3b shows the DSC curves during heating to 250 °C at a rate of 10 °C/min and after the isothermal crystallization at 170 °C for 5 h for all the specimens. Similar to the nonisothermal DSC, the suppressing effect of OMG is observed with all  $T_m$ s values shifting to lower temperatures with an increase in the OMG percentage. Furthermore, the specimens from LD0 to LD3 exhibit three melting peaks. The first peak (at a lower temperature) is ascribed to the melting of HC, while the second and third peaks are ascribed to the melting of SC. However, for the specimens from LD3.5 to LD5, no HC melting peak is observed. This indicates the total suppressing effect of OMG on HC formation in specimens with OMG contents higher than 3%. This suppression was expected in view of the visible decrease in HC melting peaks with increasing the OMG content (this will be further explained in the discussion of Fig. 5). In contrast, the melting peaks of SC exhibit continuous growth with increasing the OMG content in the specimens, showing an opposite trend compared to that of HC.

To compare the results at  $T_c = 170$  °C, namely, the enhancement of SC formation and the suppression of HC formation, the specimens were examined at both  $T_c = 160$  °C and  $T_c = 180$  °C for the same duration of 5 h. Since at lower temperatures HC formation is promoted over SC [28, 29], there was a need to examine the effects of OMG at  $T_c = 160$  °C, while at a higher  $T_c$ , that is  $T_c = 180$  °C, the

**Fig. 2** **a** Experimentally measured glass transition temperature ( $T_g$ ) with estimated  $T_g$  and the cold crystallization temperature ( $T_{cc}$ ). **b** Melting temperatures ( $T_{m,HC}$  and  $T_{m,SC}$  for homocrystals and stereocomplex crystals, respectively) obtained from the second heating DSC run as a function of the OMG content (%)



effect of OMG can be observed on SC only without the interference of HC formation, even with a long duration of 5 h. For the case of  $T_c = 160^\circ\text{C}$ , Fig. 3a shows the DSC curves during heating to  $250^\circ\text{C}$  at a rate of  $10^\circ\text{C}/\text{min}$  after isothermal crystallization at  $160^\circ\text{C}$  for 5 h for all the specimens. The curves follow the same trend observed for the specimens annealed at  $T_c = 170^\circ\text{C}$ , the SC melting peaks increase, and the HC melting peaks decrease with increasing the OMG content in the specimens. Nevertheless, a complete disappearance of the HC peak is not achieved, even for LD5, the specimen with the highest content of OMG (5%), confirming the prevalence of HC formation over SC at relatively lower crystallization temperatures. Moreover, Fig. 3c shows the case of  $T_c = 180^\circ\text{C}$  after isothermal crystallization for 5 h for all the specimens. Unlike  $T_c = 160^\circ\text{C}$  and  $T_c = 170^\circ\text{C}$ , for  $T_c = 180^\circ\text{C}$  no HC peak is observed for any of the specimens, indicating that SC formed exclusively which allows the consideration of the effects of OMG on SC solely without interference by HC formation. Even for this case, the same trend of enhanced crystallization was observed where SC melting peaks increased with increasing the OMG content in the specimens. For the detailed results of the isothermal DSC measurements at  $T_c = 160^\circ\text{C}$ ,  $170^\circ\text{C}$  and  $180^\circ\text{C}$ , refer to Table S2 in the supporting information, which lists the values of  $T_m$ ,  $\Delta H_m$ ,  $\phi_{HC}$ , and  $\phi_{SC}$  for all the specimens.

Notably, the duality of the SC melting behavior observed in the split of the melting peaks, especially for  $T_c = 170^\circ\text{C}$  (except for LD5) and for  $T_c = 180^\circ\text{C}$  (LD0-LD1.5), was addressed in our previous work [14] as the effect of secondary crystallization. In Fig. 2 of reference [14], the isothermal crystallization at  $T_c = 170^\circ\text{C}$  for PLLA/PDLA (50/50) was shown for different durations, from 1 min to 5 h. This result indicates the precedence of  $SC_2$  (SC melting at a higher temperature) over  $SC_1$  (SC melting at a lower

temperature). Therefore, when comparing the different  $T_c$ s in Fig. 3, at higher  $T_c$ s ( $170^\circ\text{C}$  and  $180^\circ\text{C}$ ), SC formation is promoted, so  $SC_2$  is formed primarily, and then  $SC_1$  (the same crystalline structure as  $SC_2$  but in a smaller crystallite) is formed as a result of secondary crystallization. However, at a lower  $T_c$  ( $160^\circ\text{C}$ ), after the initial SC formation, priority is given to the HC. This is further confirmed by the non-isothermal DSC results in Fig. 1, where only one SC melting peak is observed. Therefore, for the cases of  $T_c = 170^\circ\text{C}$  and  $180^\circ\text{C}$ , the reported values for SC, as shown in Table S2, are split into two:  $SC_1$  and  $SC_2$ . However, for simplification purposes,  $\Delta H_m$  and  $\phi_{SC}$  are presented as the summation of both  $SC_1$  and  $SC_2$  values. In Table S2,  $T_{m,SC}$  is reported as the higher melting temperature ( $T_{m,SC2}$ ), as it is attributed to the larger crystallite. On the other hand, at  $T_c = 160^\circ\text{C}$ , the melting peak of SC is mainly one peak, as shown in Fig. 3a, preceded by a slight crystallization (exothermic) peak in some cases, which was taken into consideration when estimating the baseline and calculating  $\Delta H_m$  and  $\phi_{SC}$ .

Using Eqs. 1–3, the degree of crystallinity ( $\phi$ ) was calculated from the DSC curves in Fig. 3 and plotted as a function of the OMG content in the specimens, as shown in Fig. 4, where  $\phi_{HC}$  and  $\phi_{SC}$  are plotted in Fig. 4a–c for  $T_c = 160^\circ\text{C}$ ,  $T_c = 170^\circ\text{C}$ , and  $T_c = 180^\circ\text{C}$ , respectively. The total crystallinity ( $\phi_{HC} + \phi_{SC}$ ) is displayed for all  $T_c$ s values in Fig. 4d. Additionally, the thermodynamic quench depth ( $\Delta T = T_m - T_c$ ) is also plotted in Figure 4a–c.

First, for HC, for the case of  $T_c = 160^\circ\text{C}$  (Fig. 4a),  $\phi_{HC}$  had the highest value for all specimens at all  $T_c$ s values before following a decreasing trend with increasing the OMG content. Although a discontinuity in the trend was observed at LD2, the rate of decrease remained almost the same before and after this drop. This decrease in  $\phi_{HC}$  was accompanied by a decrease in  $\Delta T_{HC}$ , that is, a decrease in

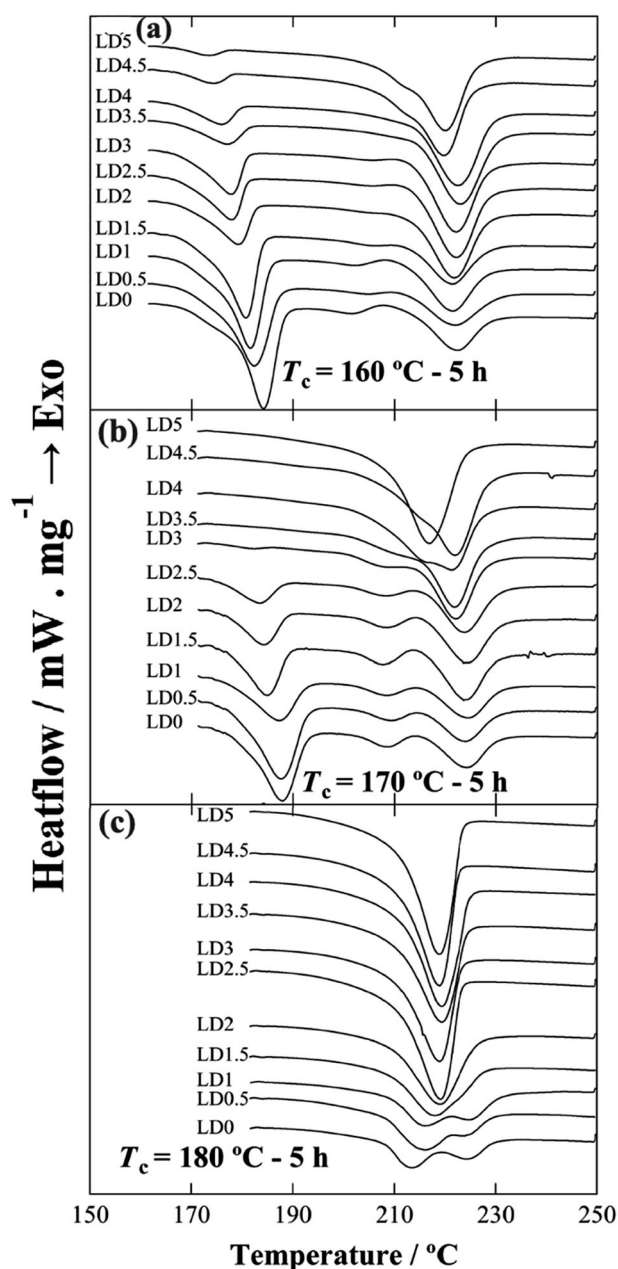


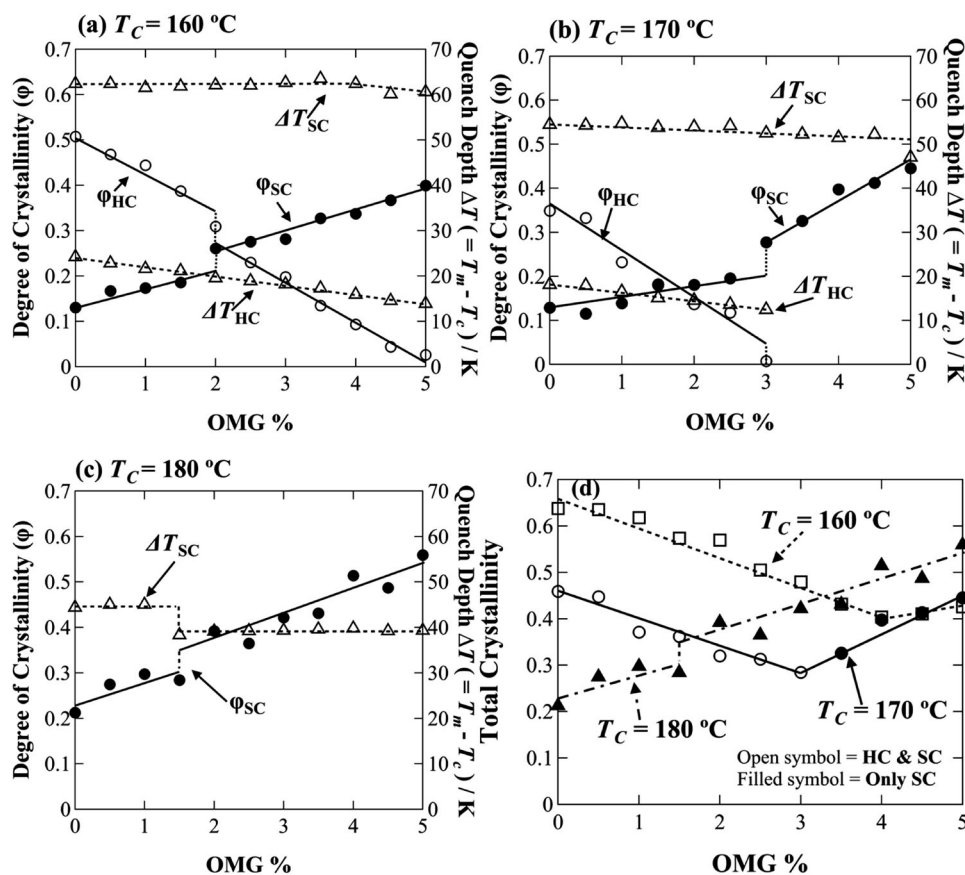
**Fig. 3** DSC curves during the heating to 250 °C (10 °C/min) after the isothermal crystallization for 5 h at 160 °C (a), 170 °C (b) and 180 °C (c) for the PLLA/PDLA (50/50) blend specimens with different OMG contents

the thermodynamic driving force of HC crystallization due to the higher loadings of OMG. Next, for  $T_c = 170$  °C,  $\phi_{HC}$  also exhibited a decreasing tendency at a higher rate (as shown in Fig. 4b) than that for  $T_c = 160$  °C, until reaching LD3. This was coupled with the decrease in  $\Delta T_{HC}$  which seemed to reach a pivotal point at LD3 with the lowest  $\phi_{HC}$  value, after which HC did not form in the specimens LD3.5-LD5. Then, for  $T_c = 180$  °C, HC was not formed in any of the specimens, even with a long isothermal duration, indicating that this  $T_c$  is too high for its formation.

Second, regarding SC, for  $T_c = 160$  °C (Fig. 4a),  $\phi_{SC}$  started at a much lower value, 4-fold lower than  $\phi_{HC}$ , and gradually increased with increasing the OMG content in the specimens. Similar to  $\phi_{HC}$ ,  $\phi_{SC}$  witnessed a jump at LD2, but similar to  $\phi_{HC}$ , the rate of  $\phi_{SC}$  increase did not change before and after LD2. In Fig. 4a, the observed gaps in  $\phi_{HC}$  and  $\phi_{SC}$  both occurred at LD2, indicating a trade-off correlation induced by the facilitated stereocomplexation and hindrance of HC formation due to  $T_m$  suppression along with the OMG plasticizer effect in decreasing the viscosity and increasing chain mobility [30]. Moreover,  $\Delta T_{SC}$  in Fig. 4a exhibits an almost constant tendency, indicating that the increase in  $\phi_{SC}$  was caused by OMG, and was not thermodynamically driven. For  $T_c = 170$  °C,  $\phi_{SC}$  showed a similar trend to the case of  $T_c = 160$  °C, steadily increasing until LD3 where it increased substantially followed by a noticeably higher rate of increase. This acceleration in SC formation, starting with LD3.5, may be triggered by the total suppression of the HC formation, which allowed further SC formation. Surprisingly, the values of  $\Delta T_{HC}$  and  $\Delta T_{SC}$  in Fig. 4b both decreased with increasing the OMG content in the specimens, with  $\Delta T_{HC}$  decreasing at a faster rate. This similar decreasing trend had opposing effects on suppressing and promoting HC and SC crystallization, respectively. Then, for  $T_c = 180$  °C (Fig. 4c), where only SC formed for all the specimens,  $\phi_{SC}$  showed an increasing trend with increasing the OMG content in the specimens. However,  $\Delta T_{SC} (= T_{m,SC2} - T_c)$  shows a constant trend with a sudden decrease at LD1.5 due to the merging of the double melting peak of SC into a single peak. Thus, the promotion of SC formation was a direct effect of OMG and its role in lowering the surface free energy of the crystallite surface comprising the chain folds by facilitating chain folding. It is worth noting that  $\phi_{SC}$  of LD0 had the same value for  $T_c = 160$  °C and 170 °C (but it was twofold higher at  $T_c = 180$  °C) indicating its independence of  $T_c$  at the lower crystallization temperatures. In contrast,  $\phi_{HC}$  was significantly greater for  $T_c = 160$  °C than for  $T_c = 170$  °C, reaffirming the favored formation of HCs at relatively lower  $T_c$ s. Nonetheless, both  $\phi_{HC}$  and  $\phi_{SC}$  were dependent on the OMG content in the specimens, and they exhibited opposite behaviors, as presented above.

Finally, the total crystallinity is shown in Fig. 4d. This reflects the above-mentioned results. At  $T_c = 160$  °C, the total crystallinity, obtained by the summation of  $\phi_{HC}$  and  $\phi_{SC}$ , decreased until reaching LD4 and then slightly increased until reaching LD5, indicating that the HC decreased at a faster rate compared to the increase of SC, with the higher OMG content in the specimens. A similar trend was observed for  $T_c = 170$  °C, where the crystallinity decreased (at the same rate as  $T_c = 160$  °C) until reaching LD3 and then increased until reaching LD5 at a faster rate compared to both  $T_c = 160$  °C and 180 °C. However, for

**Fig. 4** The degree of crystallinity for both HC ( $\phi_{\text{HC}}$ ) and SC ( $\phi_{\text{SC}}$ ), for the cases of (a)  $T_c = 160^\circ\text{C}$ , (b)  $T_c = 170^\circ\text{C}$  and (c)  $T_c = 180^\circ\text{C}$ , in relation to the quench depth. These values were evaluated from the DSC results ( $\Delta H_m$ ). **d** The total degree of crystallinity after 5 h of isothermal crystallization at  $160^\circ\text{C}$ ,  $170^\circ\text{C}$  and  $180^\circ\text{C}$  for the PLLA/PDLA (50/50) blend specimens with different OMG contents



$T_c = 180^\circ\text{C}$ , the crystallinity followed an increasing trend from the start, due to the lack of the HC formation at such a high  $T_c$ . The total crystallinity for  $T_c = 180^\circ\text{C}$  was three times lower than at  $T_c = 160^\circ\text{C}$  due to the shallower quench depth; however, the total crystallinity increased with increasing the content of OMG. As shown in Fig. 4d, for  $T_c = 180^\circ\text{C}$ , the total crystallinity surpassed that for  $T_c = 160^\circ\text{C}$  and  $170^\circ\text{C}$  for specimens LD4-LD5. Additionally, it is noteworthy that the total crystallinity of LD5 is greater than that of LD0 for  $T_c = 170^\circ\text{C}$ . While the latter is a mix of HC and SC, the former is SC only. Therefore, the exclusive formation of SC was accomplished with a higher degree of crystallinity for LD5.

Figure 5 presents the plots of  $T_{m,\text{SC}}$  and  $T_{m,\text{HC}}$  as a function of the OMG content. Here, the  $T_{m,s}$  are obtained from the DSC curves displayed in Fig. 3 for the specimens isothermally crystallized at  $T_c = 160^\circ\text{C}$ ,  $170^\circ\text{C}$  and  $180^\circ\text{C}$  for 5 h. A decreasing trend is observed for all values of  $T_{m,s}$  due to the effect of OMG with the exception of  $T_{m,\text{SC}}$  in the case of  $T_c = 160^\circ\text{C}$ , where it seems to follow an almost constant trend, irrespective of the OMG content. Nonetheless, the decrease in  $T_m$  is more pronounced in the case of HC, where  $T_{m,\text{HC}}$  exhibited a steady and parallel decrease for both  $T_c = 160^\circ\text{C}$  and  $170^\circ\text{C}$ . Note here that for  $T_c = 180^\circ\text{C}$ , HC was not formed; hence, only  $T_{m,\text{SC}}$  is shown.

Figure 6 shows the heat flow curves during the isothermal crystallization of specimens LD0, LD1, LD2, LD3, LD4 and LD5 for 5 h at  $T_c = 160^\circ\text{C}$  (a),  $T_c = 170^\circ\text{C}$  (b) and  $T_c = 180^\circ\text{C}$  (c), and their respective enthalpies of crystallization ( $\Delta H_c(t)$ ) as a function of time are presented in Fig. 6d–f, respectively. Figure 6a–c clearly demonstrate the difference between the higher and lower crystallization temperatures as a distinct trend is observed in the crystallization peaks, marked by a noticeable narrowing and sharpening of the peaks, not only due to the lower  $T_c$  but also the increase in the OMG content in the specimens within the same  $T_c$ . All the crystallization peaks for  $T_c = 160^\circ\text{C}$  are easily discernible compared to those for  $T_c = 170^\circ\text{C}$  and  $T_c = 180^\circ\text{C}$ , especially for the cases of LD0, LD1 and LD2, where the peaks are broader and less distinguishable. This narrowing and sharpening of crystallization peaks, such as LD5 for  $T_c = 160^\circ\text{C}$  indicate the synergistic effect of the OMG in accelerating the crystallization and lowering  $T_c$ , which significantly enhanced the crystallization by increasing the nucleation rate [31]. Additionally, for  $T_c = 170^\circ\text{C}$ , the effect of OMG had a similar influence to that of the lower  $T_c$ , with a progressive sharpening of crystallization peaks from LD0 to LD5. The same trend is observed for  $T_c = 180^\circ\text{C}$ , although the overall observation is the broadening of the peak, indicating slower

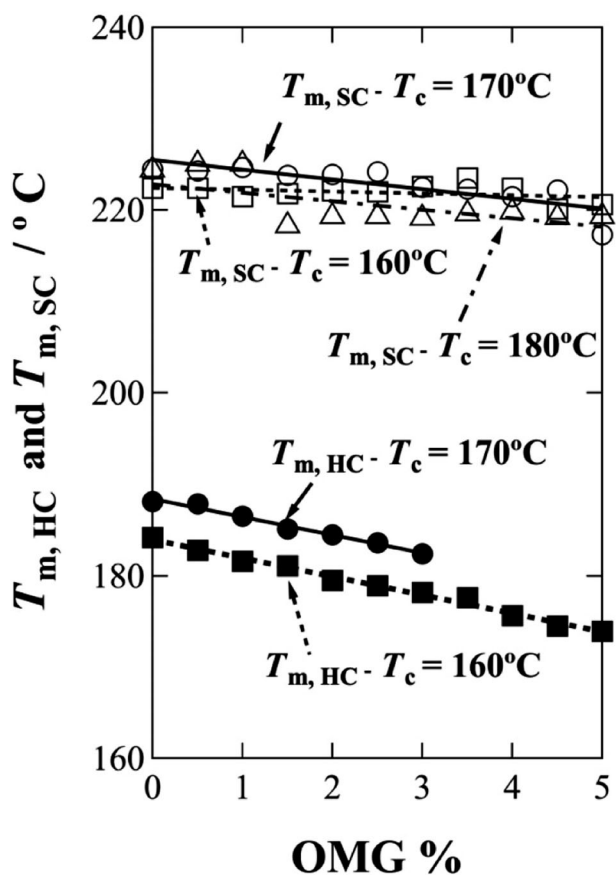


**Fig. 5** Plots of  $T_{m,HC}$  and  $T_{m,SC}$  as a function of the OMG content for the specimens isothermally crystallized at 160 °C, 170 °C and 180 °C for 5 h

crystallization processes compared to those at  $T_c = 160$  °C and 170 °C.

$\Delta H_c(t)$ , obtained by integrating the crystallization curves of Fig. 6a–c, is shown in Fig. 6d–f for  $T_c = 160$  °C, 170 °C, and 180 °C, respectively. Generally, the main observation is the steeper slope in the initial crystallization stage for  $T_c = 160$  °C compared with  $T_c = 170$  °C and 180 °C. For  $T_c = 160$  °C, all the specimens, except LD0 and LD1, almost follow the same course, and the difference among these specimens (LD3, 4, 5) is insignificant. This indicates, first, a very fast crystallization rate for the specimens from LD3 to LD5. Second, the slower crystallization observed in LD0 and LD1 suggests that the role of OMG is secondary to the role of  $T_c$  in this case. Thus, all the specimens exhibit nearly adjacent curves for the lower  $T_c$  (160 °C) compared to the higher  $T_c$ s. On the other hand, for  $T_c = 170$  °C, the specimens followed a dissimilar trend, especially during the initial stage. Here, LD4 and LD5 exhibit the highest slopes and fastest crystallization, followed by LD3, LD1, LD0 and LD2. This clear disparity in the crystallization rate between the specimens indicates the significance of the role of the OMG in accelerating the crystallization within the same  $T_c$ .

For the case of  $T_c = 180$  °C, it shows milder slopes for all the specimens compared to the lower  $T_c$ s, indicating an overall slower crystallization rate at the higher crystallization temperature [32, 33].

Furthermore, to assess the effects of OMG, the crystallization half-time ( $t_{1/2}$ ) and its inverse ( $1/t_{1/2}$ ) were evaluated from the plots of  $\Delta H_c(t)$  in Fig. 6d–f, and are shown in Fig. S1 in the supporting information. It is worth noting that  $t_{1/2}$  is the point during the crystallization time when half of the final crystallinity is completed, and its inverse indicates the crystallization rate. For  $T_c = 160$  °C, the  $t_{1/2}$  values are 29.6, 26.7, 23, 12, 15.3, and 10 min for LD0, LD1, LD2, LD3, LD4 and LD5, respectively. Then, for  $T_c = 170$  °C, the  $t_{1/2}$  values are 84.2, 63.2, 44.4, 34.1, 29.7, and 28.3 min for LD0, LD1, LD2, LD3, LD4 and LD5, respectively; while for  $T_c = 180$  °C, the  $t_{1/2}$  values are 69.4, 64.9, 49.2, 48.3, 52.5, and 56 min for LD0, LD1, LD2, LD3, LD4 and LD5, respectively. These results show that the OMG significantly shortens the crystallization time to almost the third of its highest value for both  $T_c = 160$  °C and 170 °C ( $t_{1/2}$  (LD0)  $\approx 3 t_{1/2}$  (LD5)). Note here that the exclusive formation of SC was not attained and that the degree of the total crystallinity of LD5 is much lower than that of LD0 (see Fig. 4d). On the other hand, for  $T_c = 180$  °C,  $t_{1/2}$  followed a similar trend to that for of  $T_c = 170$  °C, with decreasing values until reaching LD3, before increasing again for LD4 and LD5. This may indicate the unfavorable effect of the higher content of OMG, as excessive OMG content may result in melting point depression, although the quench depth ( $\Delta T_{SC}$ ) was observed almost constant, irrespective of the OMG content (see Fig. 4c).

#### WAXD Measurements for the PLLA/PDLA (50/50) blend specimens at $T_c = 170$ °C

To confirm the DSC results, time-resolved WAXD measurements were carried out at 170 °C for 5 h for specimens LD3, LD4 and LD5, as shown in Fig. 7. The same measurement under the same condition was performed for specimen LD0 and reported in our previous work [14] but for a shorter duration (3 h), and the results are included in Figs. 7c and 9 for comparison. It is also worth noting that the main focus was  $T_c = 170$  °C, as this is the  $T_c$  that yielded the complete suppression of HC for the specimens LD3.5–LD5 in the DSC measurements. For  $T_c = 160$  °C, the concurrent formation of both SC and HC occurred in all the specimens, and for  $T_c = 180$  °C, the SC formed exclusively in all the specimens; thus, neither  $T_c = 160$  °C nor  $T_c = 180$  °C were examined by the WAXD measurements.

Figure 7a–c show the changes in the WAXD profiles during the isothermal crystallization for specimens LD3, LD4, and LD5, respectively. LD3 in Fig. 7a exhibits the HC



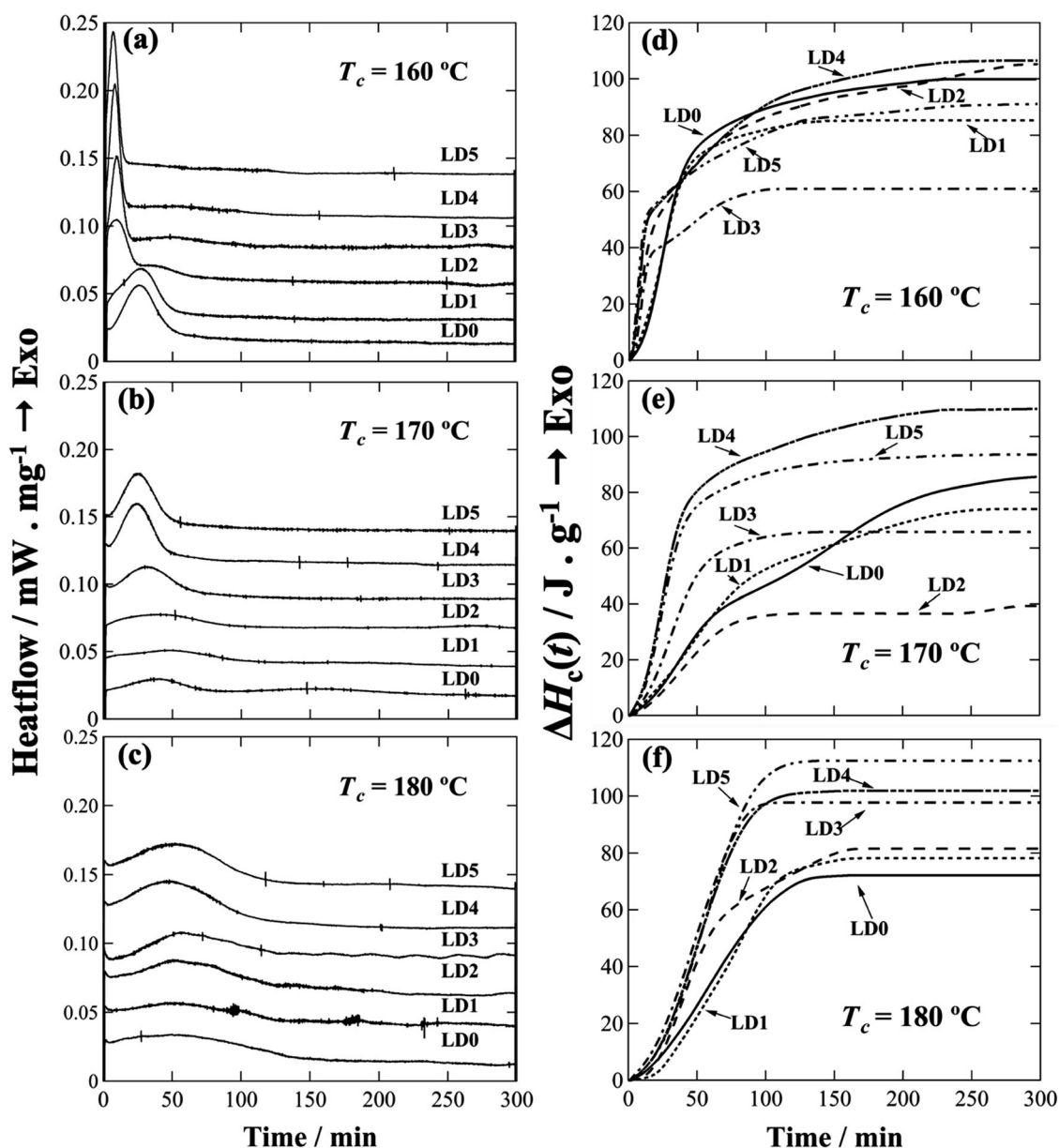


**Fig. 6** DSC curves during the isothermal crystallization at **a** 160 °C, **b** 170 °C and **c** 180 °C for the PLLA/PDLA (50/50) blend specimens with different OMG contents, and the resulting enthalpies of crystallization ( $\Delta H_c(t)$ ) as a function of time ( $t$ ) (**d–f**)

diffraction peak at  $q = 12.1\text{ nm}^{-1}$  after about 2 h of isothermal crystallization at  $T_c = 170\text{ }^\circ\text{C}$ , in addition to the SC peaks at  $q = 8.5\text{ nm}^{-1}$ ,  $q = 14.8\text{ nm}^{-1}$  and  $q = 16.9\text{ nm}^{-1}$ , which are observed much earlier (after about 5 min). However, LD4 and LD5 in Fig. 7b, c, respectively, show that the SC diffraction peaks that evolved with time, until the end of the isothermal crystallization duration of 5 h, without the appearance of the HC peaks. This confirms the DSC results showing that the addition of 4 and 5% OMG to the PLLA/PDLA (50/50) blends suppressed the HC formation at  $T_c = 170\text{ }^\circ\text{C}$ . The degree of crystallinity,  $\varphi_{\text{SC}}$  and  $\varphi_{\text{HC}}$ , as a function of time (Fig. 7d) was calculated from the

WAXD profiles by the following equations [34]:

$$\varphi_{\text{HC}} = \frac{\Sigma A_{\text{HC}}}{\Sigma A_{\text{HC}} + \Sigma A_{\text{SC}} + A_a} \quad (5)$$

$$\varphi_{\text{SC}} = \frac{\Sigma A_{\text{SC}}}{\Sigma A_{\text{HC}} + \Sigma A_{\text{SC}} + A_a} \quad (6)$$

where  $A_a$  is the peak area of the amorphous halo.  $\Sigma A_{\text{HC}}$  and  $\Sigma A_{\text{SC}}$  are the summations of the peak areas of HC and SC, respectively. Peak decomposition was performed to distinguish between the amorphous and crystalline peaks, and then the degree of crystallinity ( $\varphi_{\text{SC}}$  and  $\varphi_{\text{HC}}$ ) as a function

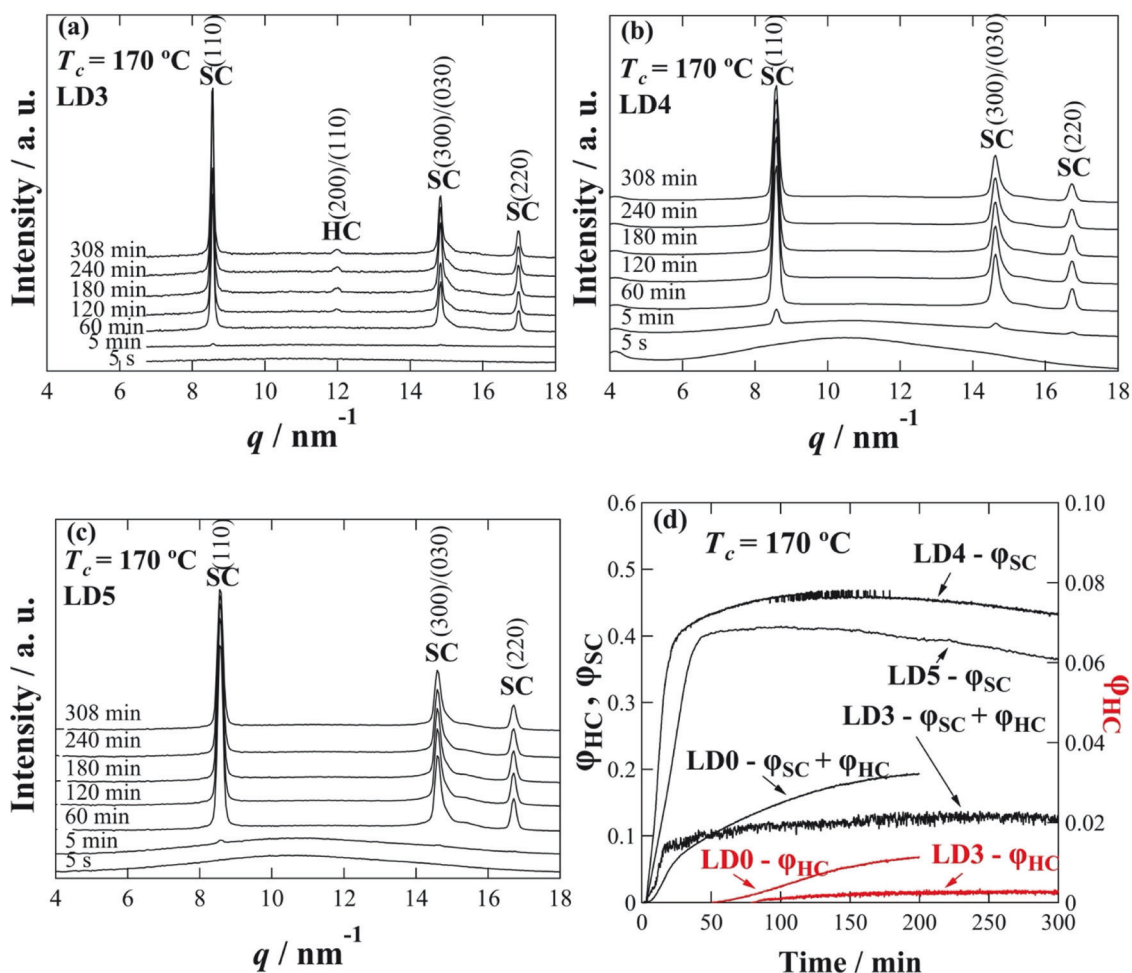


**Fig. 7** Changes in the WAXD profiles during the isothermal crystallization at 170 °C for **a** LD3, **b** LD4, and **c** LD5. **d** Temporal changes in the overall degree of crystallinity ( $\phi_{\text{HC}}$ ,  $\phi_{\text{SC}}$ ) and the expanded view of  $\phi_{\text{HC}}$  for LD0 and LD3 (red)

of time was evaluated, as shown in Fig. 7d. LD4 shows the fastest crystallization and the highest degree of crystallinity, with only SC forming. This finding aligns with Fig. 6e, which also shows the highest  $\Delta H_c(t)$ . Remarkably, the  $\phi_{\text{SC}}$  of LD4 is twofold greater than the sum of  $\phi_{\text{HC}}$  and  $\phi_{\text{SC}}$  of LD0, in addition to the much steeper slope of the initial stage of crystallization for LD4 compared to that for LD0. This attests to the ability of OMG to accelerate and facilitate the stereocomplexation of the PLLA/PDLA (50/50) blend. Moreover, LD5 shows a lower degree of crystallinity than LD4, indicating that in LD5, the OMG content is too high, leading to lower crystallization. This is also reflected in Fig. 6e, though not in the degree of crystallinity calculated from the DSC results in Fig. 4b. This may be due to partial recrystallization occurring during the heating from  $T_c = 170$  °C to 250 °C, which was facilitated by the higher loading of the plasticizer. To assess this assumption, further isothermal DSC measurements were carried out for LD5 at  $T_c = 175$  °C, 185 °C, 190 °C, 195 °C, and  $T_c = 200$  °C for 5 h. The evaluated values of  $\phi_{\text{SC}}$  and  $T_{\text{m,SC}}$  are shown in Fig. 8. The results indicate that at higher  $T_c$ s, i.e., at

175 °C–190 °C, the degree of crystallinity of LD5 is greater than that at  $T_c = 170$  °C. Additionally, in Fig. 7d, LD5 shows an unexpected decreasing tendency with increasing the crystallization duration, which was not observed for LD0 or LD3. The reason behind this decrease warrants further investigation in the future studies, to comprehensively understand the reason for this decline, albeit a small decline, in the degree of crystallinity. LD3 exhibits the lowest degree of crystallinity (see Fig. 4d), which also aligns with the DSC results for the degree of crystallinity shown in Fig. 6e, where  $\Delta H_c(t)$  of LD3 is lower than those of LD0 and LD1. A closer examination of LD3 and LD0 in Figs. 7d and 6e suggest the same tendency, that is, in the initial stage of crystallization (SC formation), LD3 has a higher rate, as proven by both DSC and WAXD. However, with increasing the duration, the crystallization of LD0 surpasses that of LD3 due to the ability of OMG to suppress the HC formation in LD3. This is clearly observed when comparing  $\phi_{\text{HC}}$  of both LD0 and LD3 in Fig. 7d (red curves). In LD0,  $\phi_{\text{HC}}$  has a much greater value than  $\phi_{\text{HC}}$  in the case of LD3.

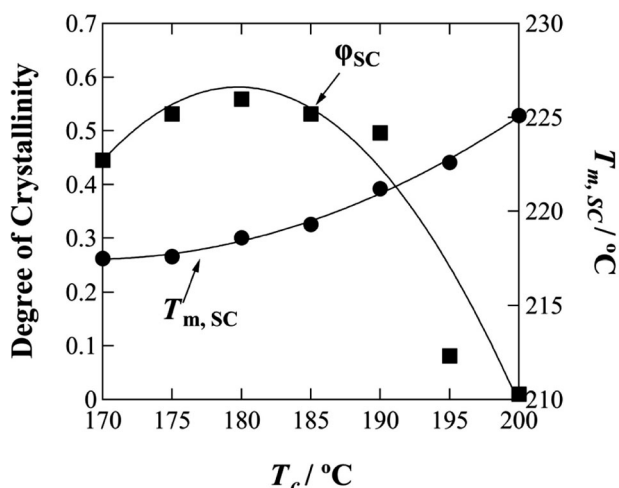


**Fig. 8** Degree of crystallinity for SC at different crystallization temperatures and the obtained melting temperatures after 5 h of isothermal crystallization for the LD5 specimen by the DSC measurements

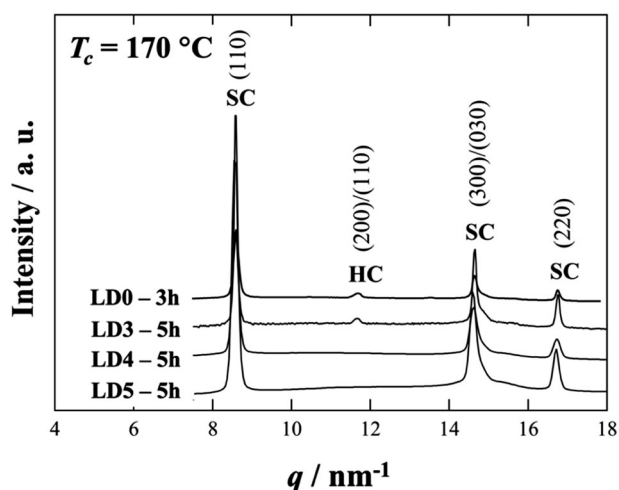


**Fig. 9** WAXD profiles after the isothermal crystallization at 170 °C for 5 h (LD3, LD4 and LD5) and that after 3 h (LD0)

Figure 9 shows the WAXD profiles after the isothermal crystallization at 170 °C for LD3, LD4, and LD5 after 5 h and that for LD0 after 3 h. This reiterates what was presented above and makes it easier to compare all the examined specimens, emphasizing that the HC diffraction peaks only appeared in LD0 and LD3. Meanwhile, LD4 and LD5 exhibit only SC diffraction peaks for the same crystallization duration as LD3 (longer than LD0).

### POM observations at $T_c = 170\text{ °C}$ for the PLLA/PDLA (50/50) blend specimens with different contents of OMG

Figure 10 shows the POM images obtained after 5 h of isothermal crystallization at  $T_c = 170\text{ °C}$  for the LD0, LD1, LD2, LD3, LD4, and LD5 specimens. The detailed images of these

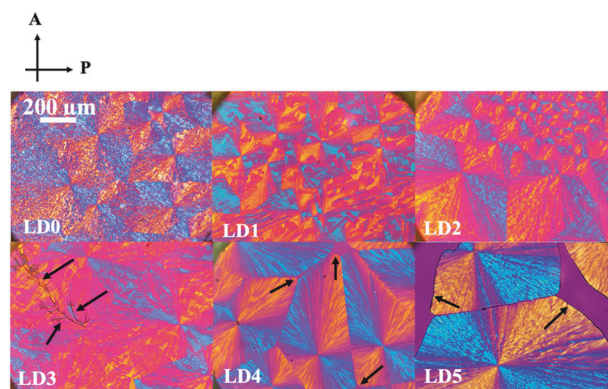


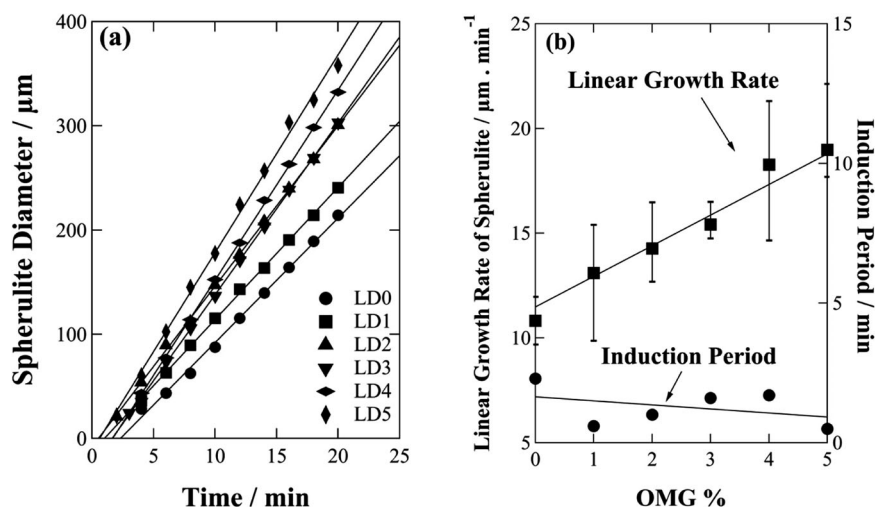
**Fig. 10** POM images obtained after the isothermal crystallization for 5 h at 170 °C for the PLLA/PDLA (50/50) specimens with different OMG contents

specimens are presented in Figures S2–S6 in the supporting information and they include the spherulite morphology during the isothermal crystallization for 5 h at  $T_c = 170\text{ °C}$ , as well as the heating process to 250 °C afterwards. The POM images of LD0, examined under the same conditions, were already available in our previous work [14], and the image of the final stage is presented in Fig. 10 for comparison.

The images in Fig. 10 show the effects of OMG on the spherulite morphology after a long duration. Considering that the specimens from LD0 to LD3 exhibit a mix of HC and SC, while the specimens LD4 and LD5 exhibit only SC, the images confirm what was proposed in our previous paper: “the HC formed within the already established SC spherulites” [14]. The spherulites in LD4 and LD5 display a clear and sharp morphology with smooth and well-defined patterns, while the spherulites in specimens LD0, LD1, LD2, and LD3 seem “filled” by the HC formation and display an indistinct appearance. Moreover, LD0 shows the most fine structures compared to the other specimens since it has the highest HC content. These fine structures decreased with increasing OMG content, leading to a more simplified morphology, such as that of LD4 and LD5, due to the suppression of HC formation.

Conversely, the increase in the OMG content in the specimens led to its aggregation in the interspherulitic regions, as indicated by the arrows in Fig. 10, for LD3, LD4, and LD5. In the case of LD5, the aggregated amount covered 15% of the observed space. This physical hindrance of spherulite growth may be the reason why the degree of crystallinity is greater in the case of LD4, as was found by the WAXD results in Fig. 7d. This indicates that a higher OMG content does not necessarily yield better results, with 5% OMG being too high and having unfavorable effects. Furthermore, the number of nuclei decreased with increasing the OMG content, where the average number obtained from at least 3 measurements was 36, 27, 22, 18, 11, and 5 for LD0, LD1, LD2, LD3, LD4 and LD5 respectively. A

**Fig. 11 a** Plots of spherulite diameter as a function of time during the isothermal crystallization at 170 °C for the PLLA/PDLA (50/50) specimens with different OMG contents. **b** Linear growth rate of spherulites as a function of the OMG content (%) and the induction period estimated from the plots in part **a**



decrease in the number of nuclei/spherulite with increasing OMG content was expected, as it is the same effect that would be observed with the increase of the crystallization temperature [35] in view of the role of OMG in  $T_m$  depression.

Nevertheless, despite the physical hindrance and lower number of nuclei, the increase in the OMG content in the specimens accelerated spherulite growth, as shown in Fig. 11. Figure 11a shows a plot of the spherulite diameters as a function of time. Linear fitting was used to evaluate the linear growth rate of the spherulites, which was subsequently plotted in Fig. 11b as a function of the OMG content in the specimens. Linear fitting also allows for the estimation of the induction period, as plotted in Fig. 11b, which was 2.3, 1, 0.6, 1.6, 1.7, and 0.5 min for LD0, LD1, LD2, LD3, LD4, and LD5, respectively. LD5, which has the shortest induction period, further verified the accelerating effect of OMG on the crystallization.

## Conclusions

The effects of loading amounts of OMG were investigated in PLLA/PDLA (50/50) blends by means of DSC, WAXD, and POM. The experimental results of both nonisothermal and isothermal DSC measurements indicate that the addition of OMG resulted in the complete suppression of the HC formation and the exclusive SC formation in the specimens with OMG contents of 3.5% or higher after isothermal crystallization at 170 °C for 5 h. This result was confirmed by WAXD, where only SC peaks were observed after isothermal crystallization at 170 °C for 5 h. In addition, the degree of total crystallinity was found to be greater for the specimen with 5% OMG than for the specimen with 0% OMG, which was crystallized at 170 °C for 5 h. This finding implies that not only did the SC form exclusively but also

that the presence of OMG actively accelerated its crystallization. Thus, it was revealed that the OMG has efficiency in the exclusive formation of SC and the suppression of HC in PLLA/PDLA (50/50) blend specimens.

**Acknowledgements** The WAXD experiments were performed under the approval of the Photon Factory (High Energy Research Organization, Tsukuba, Japan) Program Advisory Committee (Proposal No: 2022G623 and Proposal No: 2021G569).

## Compliance with ethical standards

**Conflict of interest** The authors declare no competing interests.

## References

- Jiménez, A, Peltzer, M and Ruseckaite, R. Poly(lactic acid) Science and Technology Processing, Properties, Additives and Applications, Cambridge, UK: The Royal Society of Chemistry, 2015.
- Klauss, M, Degradation of biologically degradable packaging items in home or backyard composting systems: with a special focus on the pilot scale field test for compostable packing in Kassel, Germany, Berlin, Germany: Rhombos-Verlag, 2004.
- Saeidlou S, Huneault MA, Li H, Sammut P, Park CB. Evidence of a dual network/spherulitic crystalline morphology in PLA stereocomplexes, *Polymer*. 2012;53:5816–24. <https://doi.org/10.1016/j.progpolymsci.2012.07.005>
- Li Y, Wang Y, Liu L, Han L, Xiang F, Zhou Z. Crystallization improvement of poly(L-lactide) induced by functionalized multi-walled carbon nanotubes. *J Polym Sci Part B: Polym Phys*. 2009;47:326–39. <https://doi.org/10.1002/polb.21645>
- Gámez-Pérez J, Velázquez-Infante JC, Franco-Urquiza EA, Carrasco F, Santana OO, Li MasPOCH M. Fracture behavior of quenched poly (lactic acid). *Express Polym Lett*. 2011;5:82–91. <https://doi.org/10.3144/expresspolymlett.2011.9>
- Ikada Y, Jamshidi K, Tsuji H, Hyon SH. Stereocomplex formation between enantiomeric poly(lactides). *Macromolecules*. 1987;20:904–6. <https://doi.org/10.1021/ma00170a034>
- Sin LT, Tuen BS. *Poly(lactic Acid) A Practical Guide for the Processing, Manufacturing, and Applications of PLA*. Chennai, India: William Andrew; 2019.

8. Shao J, Sun J, Bian X, Cui Y, Zhou Y, Li G, et al. Modified PLA homochiral crystallites facilitated by the confinement of PLA stereocomplexes. *Macromolecules*. 2013;46:6963–71. <https://doi.org/10.1021/ma400933v>
9. Na B, Zhu J, Lv R, Ju Y, Tian R, Chen B. Stereocomplex formation in enantiomeric polylactides by melting recrystallization of homocrystals: crystallization kinetics and crystal morphology. *Macromolecules*. 2014;47:347–52. <https://doi.org/10.1021/ma402405c>
10. Song Y, Wang D, Jiang N, Gan Z. Role of PEG segment in stereocomplex crystallization for PLLA/PDLA-b-PEG-b-PDLA blends. *ACS Sustain Chem Eng*. 2015;3:1492–1500. <https://doi.org/10.1021/acssuschemeng.5b00214>
11. Gupta A, Katiyar V. Cellulose functionalized high molecular weight stereocomplex polylactic acid biocomposite films with improved gas barrier, thermomechanical properties. *ACS Sustain Chem Eng*. 2017;5:6835–44. <https://doi.org/10.1021/acssuschemeng.7b01059>
12. Li Y, Zhao L, Han C, Xiao L. Thermal and mechanical properties of stereocomplex polylactide enhanced by nanosilica. *Colloid Polym Sci*. 2021;299:1161–72. <https://doi.org/10.1007/s00396-021-04839-0>
13. Samuel C, Cayuela J, Barakat I, Müller AJ, Raquez J-M, Dubois P. Stereocomplexation of polylactide enhanced by poly(methyl methacrylate): improved processability and thermomechanical properties of stereocomplexable polylactide-based materials. *ACS Appl Mater Interfaces*. 2013;5:11797–807. <https://doi.org/10.1021/am403443m>
14. Mahmoud NHM, Takagi H, Shimizu N, Igarashi N, Sakurai S. Significantly high melting temperature of homopolymer crystals obtained in a Poly(l-Lactic Acid)/Poly(d-Lactic Acid) (50/50) blend. *ACS Omega*. 2023;8:40482–93. <https://doi.org/10.1021/acsomega.3c05165>
15. Yu S, Zhang Y, Hu H, Li J, Zhou W, Zhao X, et al. Effect of maleic anhydride grafted poly(lactic acid) on rheological behaviors and mechanical performance of poly(lactic acid)/poly(ethylene glycol) (PLA/PEG) blends. *RSC Adv*. 2022;12:31629–38. <https://doi.org/10.1039/d2ra03513h>
16. Kulinski Z, Piorkowska E, Gadzinowska K, Stasiak M. Plasticization of Poly(l-lactide) with Poly(propylene glycol). *Biomacromolecules*. 2006;7:2128–35. <https://doi.org/10.1021/bm060089m>
17. Hu Y, Hu YS, Topolkarav V, Hiltner A, Baer E. Aging of poly(lactide)/poly(ethylene glycol) blends. Part 2. Poly(lactide) with high stereoregularity. *Polymer*. 2003;44:5711–20. [https://doi.org/10.1016/S0032-3861\(03\)00615-3](https://doi.org/10.1016/S0032-3861(03)00615-3)
18. Ljungberg N, Wesslén B. The effects of plasticizers on the dynamic mechanical and thermal properties of poly(lactic acid). *Journal of Applied Polymer Science*. 2022;86:1227–34. <https://doi.org/10.1002/app.11077>
19. Jacobsen S, Fritz HG. Plasticizing polylactide—the effect of different plasticizers on the mechanical properties. *Polym Eng Sci*. 1999;39:1153–343. <https://doi.org/10.1002/pen.11517>
20. Li H, Huneault MA. Effect of nucleation and plasticization on the crystallization of poly(lactic acid). *Polymer*. 2007;48:6855–66. <https://doi.org/10.1016/j.polymer.2007.09.020>
21. Diep PTN, Masatsugu M, Doi M, Takagi H, Shimizu N, Igarashi N, et al. Effects of a special diluent as an agent of improving the crystallizability of poly(L-lactic acid). *Polym J*. 2019;51:283–94. <https://doi.org/10.1038/s41428-018-0152-5>
22. Diep PTN, Takagi H, Shimizu N, Igarashi N, Sasaki S, Sakurai S. Effects of loading amount of plasticizers on improved crystallization of poly (L-lactic acid). *J Fiber Sci Technol*. 2019;75:99–111. <https://doi.org/10.2115/fiberst.2019-0013>
23. L Taiyo Kagaku Co., What is Chirabazol, Taiyo Kagaku Co.,Ltd., 2018. [Online]. Available: [https://www.taiyokagaku.com/lab/cosmetics\\_chemical/chirabazol/](https://www.taiyokagaku.com/lab/cosmetics_chemical/chirabazol/). [Accessed 7 December 2023].
24. Xie Q, Guo G, W Lu, Sun C, Zhou J, Zheng Y, et al., Polymorphic homocrystallization and phase behavior of high-molecular-weight Poly(L-lactic acid)/poly(D-lactic acid) racemic mixture with intentionally enhanced stereocomplexation ability via miscible blending, *Polymer*, 201, 2020. <https://doi.org/10.1016/j.polymer.2020.122597>
25. Tsuji H, Ikada Y. Properties and morphologies of poly(l-lactide): 1. Annealing condition effects on properties and morphologies of poly(l-lactide). *Polymer*. 1995;36:2709–16. [https://doi.org/10.1016/0032-3861\(95\)93647-5](https://doi.org/10.1016/0032-3861(95)93647-5)
26. Tsuji H, Horii F, Nakagawa M, Ikada Y, Odani H, Kitamaru R. Stereocomplex formation between enantiomeric poly(lactic acid)s. 7. Phase structure of the stereocomplex crystallized from a dilute acetonitrile solution as studied by high-resolution solid-state carbon-13 NMR spectroscopy. *Macromolecules*. 1992;26:4114–8. <https://doi.org/10.1021/ma00042a011>
27. Garlotta D. A literature review of Poly(Lactic Acid). *J Polym Environ*. 2001;9:63–84. 10.1023/A:1020200822435
28. Tsuji H, Tezuka Y. Stereocomplex Formation between Enantiomeric Poly(lactic acid)s. 12. Spherulite Growth of Low-Molecular-Weight Poly(lactic acid)s from the Melt. *Biomacromolecules*. 2004;5:1181–6. <https://doi.org/10.1021/bm049835i>
29. Yin Y, Liu G, Song Y, Zhang X, de Vos S, Wang R, et al. Formation of stereocomplex in enantiomeric poly(lactide)s via recrystallization of homocrystals: An in-situ X-ray scattering study. *Eur Polym J*. 2016;82:46–56. <https://doi.org/10.1016/j.eurpolymj.2016.05.033>
30. Shirai MA, Müller CMO, Grossmann MVE, Yamashita F. Adipate and citrate esters as plasticizers for poly(lactic acid)/thermoplastic starch sheets. *J Polym Environ*. 2015;23:54–61. <https://doi.org/10.1007/s10924-014-0680-9>
31. Xu Y, Wang Y, Xu T, Zhang J, Liu C, Shen C. Crystallization kinetics and morphology of partially melted poly(lactic acid). *Polym Test*. 2014;37:179–85.
32. Abe H, Kikkawa Y, Inoue Y, Doi Y. Morphological and kinetic analyses of regime transition for poly[(s)-lactide] crystal growth. *Biomacromolecules*. 2001;2:1007–14. <https://doi.org/10.1021/bm015543v>
33. Sánchez FH, Mateo JM, Romero Colomer FJ, Sánchez MS, Gómez Ribelles JL, Mano JF. Influence of Low-Temperature Nucleation on the Crystallization Process of Poly(l-lactide). *Biomacromolecules*. 2005;6:3283–90. <https://doi.org/10.1021/bm050323t>
34. Pandey AK, Takagi H, Igarashi N, Shimizu N and Sakurai S, Enhanced formation of stereocomplex crystallites in Poly(L-lactic acid)/ Poly(D-lactic acid) blends by silk fibroin nanodisc, *Polymer*, 229, 2021. <https://doi.org/10.1016/j.polymer.2021.124001>
35. Ma B, Wang X, He Y, Dong Z, Zhang X, Chen X, et al. Effect of poly(lactic acid) crystallization on its mechanical and heat resistance performances. *Polymer*. 2021;212:123280 <https://doi.org/10.1016/j.polymer.2020.123280>

**Publisher's note** Springer Nature remains neutral with regard to jurisdictional claims in published maps and institutional affiliations.

Springer Nature or its licensor (e.g. a society or other partner) holds exclusive rights to this article under a publishing agreement with the author(s) or other rightsholder(s); author self-archiving of the accepted manuscript version of this article is solely governed by the terms of such publishing agreement and applicable law.